Adaptive Attitude Control for Long-Life Space Vehicles

ARTHUR R. TAYLOR*
General Electric Company, Binghamton, N. Y.

An attitude control system using reaction jet actuators is optimally efficient and reliable when fuel consumption is minimized and the total number of thruster firings for a given mission is minimized. Fixed gain rate compensated systems provide optimal performance for a single condition of bias acceleration disturbance and cannot operate effectively when unpredictable plant changes occur. A control law for a single-axis adaptive attitude control system is developed assuming that a constant bias acceleration disturbance is acting on the vehicle between thruster operations. Computation of the controlled variable, thruster on time, requires measurement of elapsed time between vehicle crossings of attitude thresholds. Controller gain is recomputed after each operation. The control system has three modes: adaptive, return, and backup, with the latter two modes being designed so that convergence to adaptive mode operation always occurs. System simulation shows that optimal performance is achieved over a wide range of bias acceleration disturbances and that optimal performance can be maintained despite plant gain changes.

Nomenclature

I_v = vehicle moment of inertia, slug-ft^2
t_c, t_i, t_o = measured times between threshold crossings, sec
t_{on} = thruster "on" time, sec
T = thruster torque, ft-lb
α = control acceleration, rad/sec^2
θ = general attitude from reference, radians
θ_P = controller attitude constant, radians
θ_M = attitude threshold defining controller deadband, radians
θ_C = separation between attitude thresholds, radians
$\dot{\theta}$ = angular rate, rad/sec
$\ddot{\theta}$ = angular acceleration due to disturbance torque, rad/sec^2
ω_1 = angular rate preceeding control pulse, rad/sec
ω_2 = angular rate following control pulse, rad/sec

Introduction

A SATELLITE attitude controller is a system designed to maintain the angular position of a space vehicle with respect to a fixed reference. It must compensate for angular disturbance torques which are present due to solar radiation pressure, magnetic fields, aerodynamic pressure, internal mass shifts, and gravity gradients.

The single-axis system considered herein maintains vehicle attitude by operating reaction jets to apply a constant correction torque about the controlled vehicle axis when in the "on" state. The energy applied in each thruster actuation is controlled by precisely adjusting the thruster on time, t_{on}. The design objectives are to minimize fuel consumption and the number of thruster operations.

The system is to utilize attitude error information and provide a control torque to the vehicle when the attitude error signal exceeds the specified accuracy limitation of the system. The controller deadband, or region in which no control action is taken, is twice the system's accuracy limitation, assuming the accuracy limits are symmetrical about the desired attitude.

Presented as Paper 69-945 at the AIAA Aerospace Computer Systems Conference, Los Angeles, Calif., September 8–10, 1969; submitted August 29, 1969; revision received February 19, 1970. In later work, under Contract NAS5-10423 to NASA, a 3-axis adaptive control computer was built to mechanize the system control law and operate with an analog computer in a closed loop.[1]

* Development Engineer, Avionic Controls Department.

A block diagram of a lead-lag compensated system appears in Fig. 1. Rate information is provided by differentiating the attitude error signal. A pseudo-rate compensated system appears in Fig. 2. Rate information here is provided by integrating the nominal control acceleration, which is applied to the vehicle by the thrusters.[2] These fixed gain systems cannot correct for degradation of thruster torque level, which may occur suddenly or gradually, or slow changes in vehicle moment of inertia due to changes in vehicle size or configuration, as for example, when a large antenna array is deployed. Effective operation in the presence of such changes requires some capability to adapt the controller gain. Moreover, these systems provide optimum performance, in terms of fuel efficiency and thruster firing frequency, for only one fixed condition of disturbance torque, whereas in long-life missions the environment may vary over a wide but predictable range.

The performance of both of these systems is illustrated in Figs. 3 and 4 for very low and very high disturbance torques. The trajectory of the vehicle is shown in attitude-time space with the controller deadband represented by the parallel lines. Each thruster actuation is shown, as the controller deadband is reached, with an arrow indicating the direction of the applied control torque which is much greater than the disturbance torque, so t_{on} is small in comparison with the time within the controller deadband. In Fig. 3 the minimum control acceleration is imparted to the vehicle with each actuation, resulting in return pulses being successively fired at alternate sides of the controller deadband. Fuel is wasted, and the thruster firing frequency is high. In contrast, the desired vehicle trajectory for this disturbance is shown by the dotted line. In Fig. 4 the thruster firing frequency is higher than that for the optimum response, shown by the dotted line. For efficient performance over a wide range of disturbance torques, a technique is required which optimizes each thruster firing such that the time within the controller deadband is maxi-

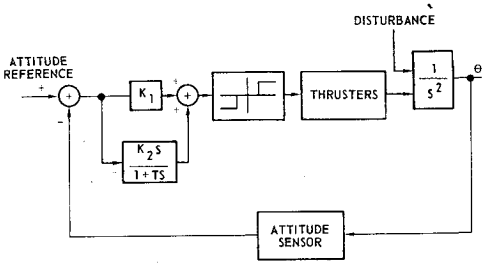

Fig. 1 Fixed gain lead-lag compensated system.

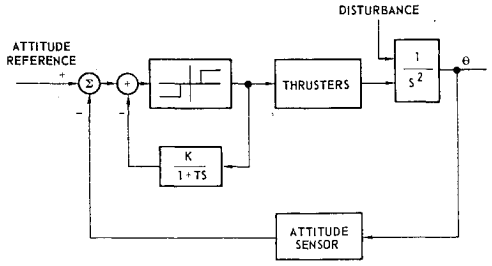

Fig. 2 Fixed gain pseudo-rate compensated system.

mized. An adaptive capability is also needed to compensate for plant variations.

The adaptive control system described herein uses a measurement of bias acceleration (angular acceleration due to disturbance torque) in computations which determine t_{on}, and also recomputes the controller gain after each actuation. An alternate system computation is used when the controller deadband is crossed and a return pulse is required. This computation uses rate information and is required to ensure stability and to maintain vehicle operation within the control deadband under some conditions. A backup system is required for start-up or acquisition capability and to provide convergence to the optimal controller under all conditions.

Derivation of Control Laws

The Adaptive Mode

The controller under consideration is designed to provide optimum performance assuming that a constant bias acceleration acts upon the vehicle. This assumption is justified because for most mission conditions the bias acceleration disturbance changes very little during the time between thruster actuations.

To achieve optimal performance it is necessary to control the energy released in the control pulse such that the depth of the resulting parabolic trajectory extends to an attitude very near, but not reaching, the opposite side of the attitude deadband. Crossing the attitude deadband completely requires a return pulse in the same direction as the bias acceleration with a resulting loss of fuel efficiency. The change in vehicle angular momentum which occurs during the thrust pulse is described by $T \cdot t_{on} = I_v \cdot \Delta\dot{\theta}$ or $t_{on} = \Delta\dot{\theta}/\alpha$, where $\alpha = T/I_v$ is the control acceleration, or the plant constant, and assuming that $\alpha \gg \ddot{\theta}$. Under these conditions the control variable is

$$t_{on} = (|\omega_1| + |\omega_2|)/\alpha \tag{1}$$

For an analytical determination of t_{on}, ω_1 must be measured and ω_2 must be identified. To identify ω_2 let us consider the equation of motion describing the optimum trajectory.

$$\theta(t) = \theta_0 + \dot{\theta}_0 t - \ddot{\theta}t^2/2 \tag{2}$$

Differentiating Eq. (1) twice with respect to t

$$d\dot{\theta}/dt = -\ddot{\theta} \tag{3}$$

or

$$d\dot{\theta}/d\theta \cdot d\theta/dt = -\ddot{\theta} \tag{4}$$

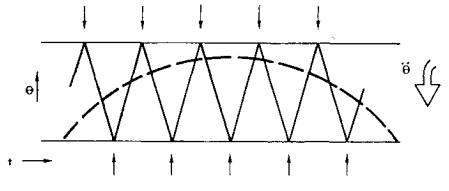

Fig. 3 Nonoptimal controller performance in low disturbance torque environment.

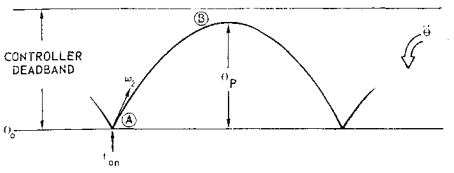

Fig. 4 Nonoptimal controller performance in high disturbance torque environment.

Hence

$$\dot{\theta}d\dot{\theta} = -\ddot{\theta}d\theta \tag{5}$$

Integrating over the trajectory in Fig. 5 from point (A) to point (B) provides the solution for ω_2 as

$$\omega_2 = (2\ddot{\theta}\theta_P)^{1/2} \tag{6}$$

ω_2, the desired rate after the control pulse, is a function of the bias acceleration, $\ddot{\theta}$. The value of θ_P is a constant, to be chosen as a function of the controller attitude deadband and other requirements of the vehicle and mission, such as the rate of change of the plant parameters and bias torque environment.

The real time computation of t_{on} requires measurements of $\ddot{\theta}$ and ω_1. A two threshold mechanization is necessary, on each side of the controller attitude deadband, to make these measurements in the design environment. The thresholds and the time intervals used for this purpose are identified in Fig. 6.

For the purposes of the theoretical development it is assumed that an initial parabolic vehicle trajectory occurs within the controller attitude deadband. This trajectory is described by $\theta(t) = -\theta_M + \dot{\theta}_0 t - \ddot{\theta}t^2/2$. Note that in the general case, the initial rate, $\dot{\theta}_0$, is the same as ω_2, the initial rate following a control pulse. The two vehicle crossings of the threshold $-(\theta_M - \theta_c)$ are described by

$$\theta_c = \omega_2 t_c - \ddot{\theta}t_c^2/2 \tag{7a}$$

$$\theta_c = \omega_2(t_c + t_i) - \ddot{\theta}(t_c + t_i)^2/2 \tag{7b}$$

Under the design constraint of a constant bias acceleration the vehicle trajectory is parabolic and symmetrical, in which case it is observed that $t_o = t_c$ and $\omega_1 = \omega_2$ where ω_1 is the rate immediately before the pulse occurring at the end of the trajectory. Then

$$\theta_c = \omega_1 t_o - \ddot{\theta}t_o^2/2 \tag{8a}$$

$$\theta_c = \omega_1(t_o + t_i) - \ddot{\theta}(t_o + t_i)^2/2 \tag{8b}$$

Solving simultaneously for ω_1 and $\ddot{\theta}$, we obtain

$$\ddot{\theta} = 2\theta_c/t_o(t_o + t_i) \tag{9}$$

$$\omega_1 = \theta_c(t_1 + 2t_o)/t_o(t_o + t_i) \tag{10}$$

Equations 9 and 10 provide an exact solution for the constant bias acceleration and the vehicle rate preceding the control pulse from the time measurements between threshold crossings, t_i and t_o, and the constant θ_c which is determined by the separation between the thresholds.

Computation of the control variable may now be carried out as

$$t_{on} = \frac{1}{\alpha}\left[\frac{\theta_c(t_i + 2t_o)}{t_o(t_i + t_o)} + \left(\frac{\theta_P\theta_c}{t_o(t_i + t_o)}\right)^{1/2}\right] \tag{11}$$

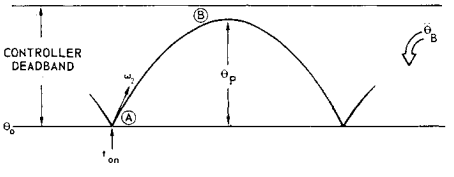

Fig. 5 Vehicle trajectory following a control pulse.

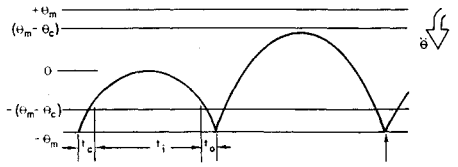

Fig. 6 The two threshold system mechanization.

To achieve the adaptive capability desired for optimum performance over the mission life (or to correct for any error in calculations of the initial plant constant) a new value of the plant constant is computed following each control pulse. After the control impulse, the expression for the vehicle trajectory is $\theta(t) = -\theta_M + \omega_2' t - \ddot{\theta} t^2/2$, where ω_2' is not necessarily equivalent to ω_2, which denotes the value required for optimum performance. At $t = t_c$,

$$\theta_c = \omega_2' t_c - \ddot{\theta} t_c^2/2 \tag{12}$$

and

$$\omega_2' = \theta_c/t_c + \ddot{\theta} t_c^2/2 \tag{13}$$

The control acceleration may be described in terms of ω_2' as,

$$\alpha' = (|\omega_1| + |\omega_2'|)/t_{on} \tag{14}$$

α' is the new value of the plant constant to be computed after each control pulse, and the computation in terms of the preceding t_{on}, angular constants, and measured time intervals is

$$\alpha' = \frac{\theta_c}{t_{on}} \left[\frac{(t_i + 2t_o)}{t_o\,(t_i + t_o)} + \frac{1}{t_c} + \frac{t_c}{t_o\,(t_i + t_o)} \right] \tag{15}$$

The control law equations describing the adaptive mode operation are given by Eqs. (11) and (15).

The Return Mode

The attitude deadband may be crossed during acquisition of the adaptive mode, or during the adaptive mode operation under conditions of rapidly changing bias torques, or when significant plant parameter changes occur. A return mode thrust pulse is then used to maintain the required attitude accuracy. Whenever this occurs, an alternate method is required to compute t_{on}. Each time a return mode thrust pulse is used, the fuel efficiency is degraded, so the major objective of the return mode operation is to reacquire the adaptive mode. This is done by reducing the absolute value of the vehicle angular momentum with the return pulse, until a parabolic trajectory is caused by the bias torque environment.

The equation for the return mode t_{on} is

$$t_{on} = 1.5\theta_c/\alpha t_o \tag{16}$$

In a zero bias torque environment, this equation effectively reduces the absolute value of vehicle rate by a factor of 0.5 each time the vehicle crosses the attitude deadband. The angular momentum would theoretically be reduced to zero in the limit, however, physical thrusters have a minimum on time, so a minimum vehicle angular momentum also exists.

In the practical situation of a finite bias torque environment, successive deadband crossings, followed by thrust pulses as computed using Eq. (16), result in an initial parabolic trajectory such as that shown in Fig. 6. This acquisition sequence is illustrated in Fig. 7. After the initial parabolic trajectory occurs, the adaptive mode is capable of controlling the vehicle with high efficiency.

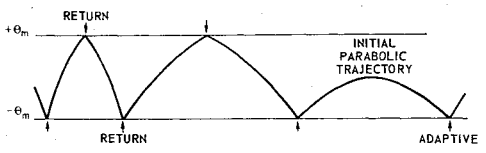

Fig. 7 Return mode acquisition sequence.

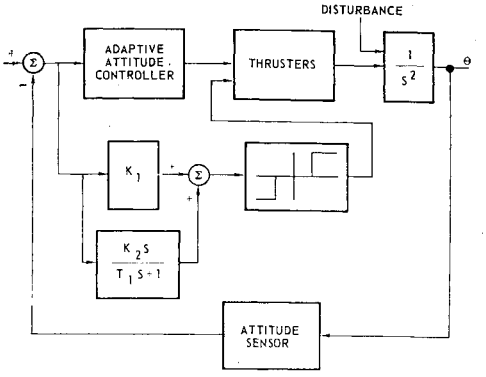

Fig. 8 Parallel system mechanization.

No new values of the plant constant may be computed after return mode pulses and the system has no adaptive capability in this mode. Thus, α is computed using Eq. (15) only after an adaptive mode pulse has been executed as obtained from Eq. (11).

The Backup System

A parallel system is needed to provide the capability to acquire the controller attitude deadband with a reasonably low vehicle rate. This parallel system might also be used to provide vehicle maneuver capability, but the present discussion is limited to acquisition of the adaptive attitude controller limit cycle from relatively high attitude and attitude rate errors.

The configuration of the adaptive system and one such parallel backup system, with the thrusters and vehicle, is shown in block diagram form in Fig. 8. The gains K_1, K_2, and the lag time constant T_1 are chosen proportional to the adaptive controller attitude deadband and the position and rate errors to be within acquisition range. In addition, the thruster on signal must command a minimum thrust pulse, such that the resulting attitude trajectory crosses the inner threshold level, $\pm(\theta_M - \theta_c)$, under the worst-case high bias-acceleration conditions. This assures acquisition of either the adaptive mode or the return mode from initial conditions within range of the backup system.

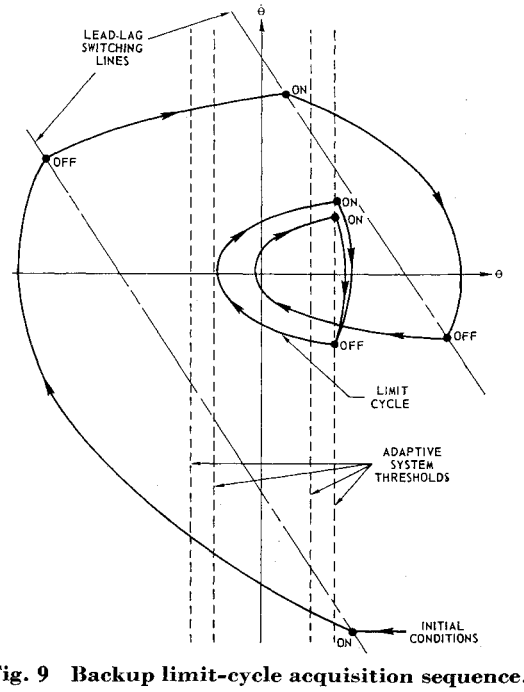

Fig. 9 Backup limit-cycle acquisition sequence.

A phase-plane diagram of a typical adaptive limit cycle acquisition sequence is shown in Fig. 9. The bias acceleration is assumed in the positive direction. The scale and slope of the lead-lag switching lines are determined by the magnitudes of K_1 and K_2. The dotted lines represent the attitude thresholds of the adaptive system, and the thruster on and off points are indicated.

Simulation of System Performance

The adaptive attitude controller performance was evaluated using a digital simulation of the controller and the controlled vehicle in a closed loop. A set of test problems was selected to demonstrate the controller capability under a wide range of spacecraft environmental conditions as well as showing the adaptive capability of the controller in the presence of plant changes. The final test problem simulated demonstrates control over a sinusoidal bias acceleration profile representative of that encountered in a synchronous, twenty-four hour orbit. The vehicle and control system parameters were chosen as representative of those for an advanced communications satellite in a synchronous orbit. $I_v = 1000$ slug-ft^2, $T = 0.2$ lb-ft, $\theta_M = 0.1°$, $\theta_c = \theta_M/5$, $|\ddot{\theta}|$ max $= (10^{-7})$ rad/sec^2, and $|\dddot{\theta}|$ max $= 7.3\ (10^{-12})$ rad/sec^3.

The system performance is evaluated with respect to fuel efficiency by comparing the fuel used by the adaptive system with the minimum fuel required to cancel the bias acceleration disturbance, computed for the total time simulated in each case. The total momentum represented by the ideal fuel expenditure is

$$T \cdot \sum_1^n t_{on} = I_v \int_o^t |\ddot{\theta}(t)|dt \tag{17}$$

or

$$\sum_1^n t_{on} = 1/\alpha \int_0^t |\ddot{\theta}(t)|dt \tag{18}$$

The actual Σt_{on}, which is found by simulating the system performance for the corresponding conditions, may then be compared to the ideal, providing a direct measure of system fuel efficiency. The actual total may be less than the ideal in some cases since the disturbance may cancel itself between controller operations with an on-off type controller.

The system performance is also evaluated for each thruster operation on the basis of how near the actual vehicle trajectory is to the desired parabolic trajectory.

Constant $\ddot{\theta}$ Case

A constant bias acceleration ($\ddot{\theta} = 10^{-7}$ rad/sec^2) was acting on the vehicle in the first case. The control acceleration, or system gain, which was initially programed into the controller was identical to the actual value determined by the vehicle moment of inertia and thruster torque. A 25% reduction in this control acceleration was programed to occur with the twelfth controller operation. This sudden change might represent a degraded thruster level or an increase in vehicle moment of inertia.

After the first adaptive mode pulse, the performance was optimal, indicating that under a constant bias acceleration disturbance, the adaptive mode computation is exact. Optimal performance was maintained until the gain change occurs with the twelfth operation. The performance was degraded for only one operation and then returned to optimal by the adaptive gain computation of α, which immediately computes the exact new gain.

The fuel required in this case was identical to the ideal during the adaptive mode operation, since there was no wasted fuel due to return pulses. The thruster firing frequency has been minimized for the time when optimal performance was maintained.

Constant $\dddot{\theta}$ Case

A constant rate of change of bias acceleration was the disturbance environment for this case. This shows the capability of the controller to operate efficiently in a rapidly changing bias acceleration environment, even though it is designed to operate in a constant bias acceleration environment. The bias acceleration starts at a value much larger than the maximum expected for the advanced communications satellite ($\ddot{\theta} = 10^{-6}$ rad/s^2), and goes through zero at a constant rate which is much higher than any rate of change of bias acceleration expected ($\dddot{\theta} = 0.2 \times 10^{-9}$ rad/s^3).

The initial value of gain programed in the controller was 50% higher than the actual control acceleration when the simulation began, so the result of the first controller operation was far from being optimal. However, the system gain was correctly computed immediately following this first operation.

Very little error is introduced into the gain computation by the changing bias acceleration, although the computation was not exact. The error in the t_{on} computations was observed as a varying error from the optimal. In a decreasing bias acceleration environment, the t_{on} computations are longer than desired, and the vehicle attitude tends to overshoot the optimal. In the increasing bias acceleration environment the computed t_{on} is too short and the vehicle attitude does not reach the optimal. The error increases as the absolute value of bias acceleration decreases. In the time period when the bias acceleration passed through zero, the vehicle crossed the attitude deadband due to the large errors and return pulses were required.

Excess fuel was used, but very little for the extreme case of bias acceleration disturbance which this case represents. The thruster firing frequency was nearly minimized for this case over the major portion of the assumed disturbance. The return pulses experienced in the time period when the bias acceleration passed through zero are unavoidable because the system control law is invalid in this region. The extra pulses do not seriously degrade the thruster firing frequency in a real mission environment since the bias acceleration disturbance does not generally pass through zero, or reverse direction very often.

Simulated Mission Profile Case

The bias acceleration disturbance for an advanced communications satellite in a synchronous orbit was approximated by $\ddot{\theta}(t) = (10^{-7}) \cos\phi t$ where $\phi = 7.27\ (10^{-5})$rad/sec for a 24 hr orbit. The system maintained near optimal performance over the range of the disturbance, having some difficulty in the region of zero bias acceleration. Control was generally maintained through zero-crossings using the return mode, however, it could happen that the computed thruster pulse was not large enough to make the vehicle cross the $(\theta_M - \theta_C)$ attitude threshold, and thus it was not possible to measure any of the times between thresholds necessary for computations. The backup system must provide control in this instance for reacquisition of the adaptive mode. The fuel efficiency was nearly ideal over the assumed disturbance. The thruster firing frequency was also minimized through most of the simulation.

Summary

The system control law provides optimal control within the design environment of a constant bias acceleration. Near-optimal performance is maintained in a general, but realistic environment, where the controller parameters are sized for the vehicle and mission environment, and a suitable backup system is present to provide stable convergence to the desired limit-cycle.

The system performance is degraded whenever a return mode pulse occurs, or when the backup system is required. This

degradation may occur whenever the rate of change of bias acceleration is so high as to make the absolute value of bias acceleration change by a large factor between consecutive thruster operations. This occurs when the bias torque disturbance passes through zero while reversing direction.

The adaptive capability of the system control law is precise in following the actual plant gain, even when performance is degraded due to a rapidly changing environment. The advantage of having this adaptive capability would be realized on an extended satellite mission as substantial fuel savings and increased system reliability due to the reduced number of thruster operations.

References

[1] "Adaptive Attitude Control System for Spacecraft Stabilization," Final Rept. ACD-8773, May 1968, General Electric Co., Binghamton, N. Y.

[2] Nicklas, J. C. and Vivian, H. C., "Derived Rate Increment Stabilization: Its Application to the Attitude-Control Problem," Technical Rept 32-69, 1961, Jet Propulsion Lab., California Institute of Technology, Pasadena, Calif.

AUGUST 1970 J. SPACECRAFT VOL. 7, NO. 8

A Spacecraft-Based Navigation Instrument for Outer Planet Missions

THOMAS C. DUXBURY*
Jet Propulsion Laboratory, Pasadena, Calif.

This article presents the results of an analytical study of various spacecraft-based data that could be used to improve solely Earth-based navigational accuracies when approaching or orbiting outer planets. Measuring the celestial directions to outer planet natural satellites can supply the needed navigation data. The satellite motion can define the celestial direction to the center-of-mass of the outer planet-satellite system more accurately than can be determined from viewing the planet itself. An instrument similar to science television cameras used on the Mariner Mars missions would be suited to produce this spacecraft-based data by viewing satellites and reference stars simultaneously. A description of an instrument producing these measurements (accurate to better than 5 arc-sec) and the applicability of these spacecraft-based data to a Grand Tour mission are also presented.

Introduction

THE positions of the outer planets during the 1970's and 1980's make various multiple-outer planet missions possible within the expected launch vehicle capabilities.[1,2] Of particular interest among possible future missions is the rare opportunity (once every 171 years) to launch spacecraft which would encounter Jupiter, Saturn, Uranus, and Neptune during a 9–13 year mission lifetime. Such outer planet missions require multiple trajectory correction maneuvers to insure the desired planet encounters. Limitations of Earth-based radio navigation capabilities at the great distances involved have led to an emphasis on developing a spacecraft-based navigation data source.[3,4] Spacecraft-based data in conjunction with Earth-based radio tracking allow more accurate control of the planet approach trajectory which significantly decreases the amount of spacecraft weight needed for trajectory correction purposes, increases mission performance, and increases the probability of mission success over that obtainable using Earth-based radio navigation only.

Radio tracking data combined with Earth ephemeris data would be used to determine the heliocentric state (position and velocity) of a spacecraft. Earth ephemeris uncertainties, tracking station location uncertainties, uncalibrated charged particle effects, and other data noise would be the major sources of error degrading the determination of the heliocentric spacecraft state when using only the Earth-based data. The determination of the target-centered spacecraft state would be degraded by this heliocentric state uncertainty and the target ephemeris uncertainty when outside the target sphere-of-influence. It is expected that Earth-based radio navigation in the mid-1970's would have the capability of determining the target-centered spacecraft state during planet approach to 0.1 arc-sec (3σ) in geocentric right ascension and declination. These uncertainties map to a spacecraft position uncertainty of 500 km at Jupiter and 3000 km at Neptune. Augmenting the Earth-based navigation data with spacecraft-based data could reduce the target-centered, spacecraft position uncertainty to ~400–1000 km (3σ) during the approach to these same planets.

This article discusses the desired information content of the spacecraft-based data and the difficulties associated with obtaining the data. Spacecraft-centered measurements of the direction to the planet center-of-mass supplies the needed trajectory information lacking from the Earth-based radio tracking data. The gaseousness of the outer planets, and the rings of Saturn makes the accuracy of planet center determination from planet limb measurements questionable. Fortunately, these gaseous planets have many natural satellites whose orbital motion can be related directly to the center-of-mass of the planet-satellite system. A television type instrument which would image these natural satellites and reference stars simultaneously to produce the desired navigation data is discussed together with the application of this data to the Grand Tour mission. The instrument re-

Presented as Paper 69-902 at the AIAA/AAS Astrodynamics Conference, Princeton, N.J., August 20–22, 1969; submitted September 8, 1969; revision received April 9, 1970. This article presents the results of one phase of research carried out at the Jet Propulsion Laboratory, California Institute of Technology, under Contract NAS 7-100, sponsored by NASA.

* Group Leader, Guidance and Control Division.